JEE Journal of Ecological Engineering

Journal of Ecological Engineering 2023, 24(2), 265–278
https://doi.org/10.12911/22998993/156886
ISSN 2299–8993, License CC-BY 4.0

Received: 2022.11.03
Accepted: 2022.12.16
Published: 2023.01.01

# Assessment of the Feasibility of Modified Chitosan Beads for the Adsorption of Nitrate from an Aqueous Solution

Zainab N. Jamka[1*], Wadood T. Mohammed[1]

[1] Department of Chemical Engineering, College of Engineering, University of Baghdad, Iraq

* Corresponding author's e-mail: zainab.mohammed1607m@coeng.uobaghdad.edu.iq

**ABSTRACT**

The objective of the current work was to investigate the effectiveness and mechanism of nitrate removal from an aqueous solution by adsorption using metal ($Zr^{4+}$)loaded chitosan and Bentonite beads (Cs-Bn-Zr). The study was carried out in a batch system, and the effect of the critical factors on the adsorption performance, such as contact time, initial nitrate anion concentration, and adsorbent dosage, were investigated. In addition, the adsorption equilibrium models of the Langmuir, Freundlich, and Temkin isotherms were evaluated. The modified adsorbent was characterized by Fourier transform infrared spectroscopy (FTIR), Field Emission Scanning Electron Microscopy (FESEM), and analysis with an energy-dispersive X-ray analyzer (EDX). The results demonstrated that at 0.2 g of CS-Bn-Zr adsorbent with an initial concentration of 50 mg/l and a contact time of 120 minutes, the maximum removal of nitrate ions was found to be 97.28%. The result demonstrated that the maximum adsorption capacity of nitrite ions on the manufactured bead was 110.46 mg/g. The Freundlich model was shown to be the most effective for the adsorbate of nitrate. The pseudo–first-order model fits the adsorption kinetic data well.

**Keywords:** chitosan, batch adsorption, nitrate, zirconium, bentonite. isotherm study.

## INTRODUCTION

Nitrate nitrogen is a substance it can be found in a variety of produced as a byproduct of the oxidation and corrosion of nitrogen-containing compounds (Ghadiri et al., 2017). Nitrate is an essential product of chemical fertilizers, sanitary sewage, and industrial wastewater. Additionally, the amount of nitrate in groundwater has increased yearly, raising concerns recently (Daneshvar et al., 2018). It has been reported that the people exposed to nitrate can develop several diseases, such as alimentary canal cancer, which is permeated by nitrate in particular (Afkhami, 2003). The blue-baby syndrome, which happens when hemoglobin transforms into methemoglobin, which is incapable of carrying oxygen, may be brought on by too much nitrate in drinking water (Golden et al., 1998). Consequently, the permissible levels of nitrate in water have been suggested in many countries to prevent these health risks. The World Health Organization has set a 50 mg/L nitrate limit for drinking water (Herschy, 2012).

As a result, many methods for eliminating nitrate from water samples have been documented; reverse osmosis (Raval et al., 2015), electro dialysis (Wang et al., 2007), chemical reduction (Hu et al., 2001), and ion exchange (Bae et al., 2002) are examples of these. Adsorption has been used to remove nitrate from water more and more frequently in recent years compared to other technologies, because of its high efficiency, ability to conserve energy, and ability to protect the environment (Liu et al., 2018; Hammadi et al., 2019). It is well-known that the type of adsorbent significantly affects the adsorption process. Numerous studies have recommended a variety of adsorbents, including organic adsorbents, inorganic adsorbents, and agricultural wastes, such as activated carbon (Sulaymon et al., 2010), silica gel (Choudhary et al., 1982), and dates pits (Hummadi, 2021). Bead-shaped adsorbents made of biopolymers are the most effective in removing

pollutants from water. It takes little effort to regenerate the beads or to extract them from the treated water afterwards (Hasmath Farzana et al., 2015). Chitosan has recently been mentioned as one of the adsorbents that can be utilized successfully to remove harmful ions (Karthikeyan et al., 2019a). Deacetylated chitin is a linear polysaccharide, well recognized as a superior biopolymeric substance. Compared to other adsorbents, this type of adsorbent has an advantage that may be summed up as follows: it is a biomaterial that can be formed into various shapes, characterized by non-toxicity, biodegradability, and biocompatibility (Hasmath Farzana et al., 2015). The main benefit of chitosan is that it contains many amino and hydroxyl groups, and the amino groups are easily protonated in acidic media (Keshvardoostchokami et al., 2021). However, certain disadvantages are associated with its use, such as poor selectivity and adsorption capacity, limited mechanical strength, and low solubility rates in acid media (Saheed et al., 2021; Ahmed et al., 2020). To improve the physicochemical properties of chitosan, various modification techniques have been proposed in recent decades. These techniques can be divided into physical and chemical modifications, such as cross-linking (AZLAN et al., 2009), metal loading (Karthikeyan et al., 2019b), and composite blend forms (Rajeswari et al., 2015).

Chitosan is cross-linked to give it mechanical strength, so it can be used in water treatment applications (Sowmya et al., 2014). Chitosan derivatives with improved characteristics are created through cross-linking reactions, which connect the macromolecular chains (enhancement of adsorption capacity and resistance under extreme media conditions, respectively) (Kyzas et al., 2015). Cross-linking of chitosan uses several common cross-linking chemicals, such as glutaraldehyde, epichlorohydrin, and ethylene glycol diglycidyl ether.

Many different alternative methods have been used to enhance the removal effectiveness and adsorption capacity of adsorbents. To solve this issue, it can be filled with various materials like multivalent metal ions. The anions are more likely to be eliminated by ions with a higher positive charge among different types of ions, such as calcium, magnesium, aluminium, and zirconium ions (Kumar et al., 2017). Zirconium is one of the many multivalent metal ions which can be combined with the materials to improve the selectivity of the adsorbent. Furthermore, Zr(IV) can be loaded onto the materials' appropriate functional groups, such as carboxyl, hydroxyl, and amino groups. Zr (IV) could bind anions like nitrate and phosphate by forming stable complexes with vacant orbits (Purbasari et al., 2022). Bentonite is a non-metallic clay mineral with a 2:1 unit cell structure of two tetrahedral silica sheets and one octahedral alumina sheet inserted between the tetrahedral sheets (Wu et al., 2001). Due to its mechanical stability, availability, affordability, and environmental friendliness, bentonite is frequently used in wastewater treatment facilities. In addition to its superior cation exchange capacity and large surface area, it also has a high removal capability for organic and inorganic contaminants (Hamid et al., 2017).

A specific kind of adsorbent was created for this study. Chitosan-bentonite-zirconium chloride composite beads are the name of the product (Cs-Bn-Zr). The primary goal of the current research is to investigate the adsorption of nitrate ions utilizing modified adsorbents. Chitosan was altered for this purpose by being combined with bentonite, and the resulting combination was loaded with zirconium chloride. The improved synthesized adsorbents were evaluated by FTIR and FE-SEM analysis and applied in a batch adsorption method. The viability of using modified chitosan adsorbents in the adsorption process was assessed by considering the removal efficiency and adsorption capacity. Therefore, this work investigated the impact of essential variables, specifically contact time, pollutant concentration, and adsorbent dosages. The study also highlighted the adsorption isotherm for the process and found the best kinetic model to describe the results obtained.

## EXPERIMENTAL WORK

### Chemicals

Chitosan powder (90% deacetylated) was purchased from chemsavers (USA). Bentonite was obtained from Iraqi Geological survey. Zirconium chloride ($ZrOCL_2 \cdot 8H_2O$) originated from BDH chemicals Ltd England. Glacial acetic acid is 99.5% from Macron Company (China). Glutaraldehyde solution 25% was bought from Thomas Baker. Sodium hydroxide pellets 98% were obtained from Orbital Company. Sodium nitrate ($NaNO_3$) is supplied by CDH. Distilled water was used to prepare all solutions.

### Preparation chitosan-bentonite-zirconium(CS-Bn-Zr) beads

The chitosan-bentonite beads were created using a previously reported method by (Sowmya et al., 2014) with modifications. Two grams of chitosan were dissolved in (100 ml) of glacial acetic acid (2% v\v) in a (250 ml) beaker. The mixture was stirred by a mixer (OS20-S) for three hours at 300 rpm at ambient temperature to obtain the homogenous gel. Then two grams of bentonite were added to the chitosan mixture and mixed for (6 hrs.) to create a uniform dispersion.

The chitosan and bentonite solution was dropped into a beaker (1 L) containing (1 M) of sodium hydroxide by burette (100 ml) and left for (20 h) to obtain viscous beads. Thereafter, the beads were washed with distilled water until the pH reached between (6.5–7.0); after that the wet beads were immersed in a Glutaraldehyde solution of 25% for (48 h) and washed with distilled water to neutralize the pH. Finally, the (CS-Bn) wet beads were placed in the zirconium chloride solution ($ZrOCL_2 \cdot 8H_2O$) (5%w\v) for (24 h) to increase the selectivity for nitrate ions and then washed several times with distilled water to remove the excess zirconium chloride. The beads were dried at room temperature. A schematic of the Cs-Bn-Zr preparation is shown in Figure 1.

### The Batch adsorption experiments

The batch adsorption experiments were performed in a 250 ml glass bottle in the shaker (1990 Germany). A specific amount of the prepared adsorbents was placed in 250 ml of sodium nitrate solution. The mixture was shaken at room temperature at a constant rotation speed of 150 rpm.

The effect of contact time (0–180 min), adsorbent dosage (0.05–0.3 g), and initial nitrate ions (50–800 mg/L) on removal efficiency and adsorption capacity were investigated throughout the study. Samples were taken periodically and filtered before analysis. After that, the samples were analyzed by a spectrophotometer at a wavelength of 220 according to Ultraviolet Spectrophotometric Screening Method described in (Rice et al., 2012).

The removal efficiency (% removal) is estimated according to the following Equation:

$$removal\% = 100 \times \frac{c_i - c_e}{c_i} \quad (1)$$

The adsorption capacity was calculated as follows:

$$adsorption\ capacity(q_e) = \frac{c_i - c_e}{m} \times v \quad (2)$$

where: $c_i$ – the initial concentration of $NO_3$ (ppm);
$c_e$ – the equilibrium concentration of $NO_3$ (ppm);
$m$ – the mass of adsorbent (g);
$v$ –the volume of solution (L).

## RESULT AND DISCUSSION

### FTIR studied adsorbent

FTIR spectra of chitosan (Cs), bentonite, and chitosan-bentonite-zirconium (Cs-Bn-Zr) bead before and after adsorption are shown in Figure 2. A broad band peak was observed in Figure 2a, which was designated for the pure chitosan overlapped stretching vibrations of the -OH and $NH_2$ groups at 3444 $cm^{-1}$. The asymmetric C-H stretching vibrational peak of the $-CH_2$ group was

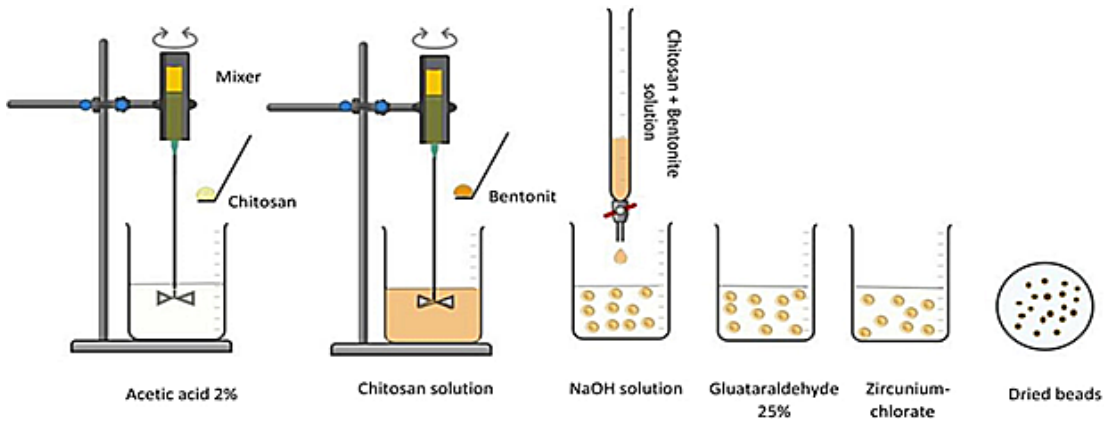


**Figure 1.** A schematic preparation of modified chitosan composite beads (Cs-Bn-Zr)

presented at 2862 $cm^{-1}$. Moreover, it can be noticed that the N-H bending vibration of NH2 and -OH was 1577 $cm^{-1}$ and 1381 $cm^{-1}$ (Karthikeyan et al., 2019c). Furthermore, the C-O-C skeletal vibrations caused the peak at 1076 $cm^{-1,}$ while the C-O stretching vibration of chitosan caused the peak at 1026 $cm^{-1}$ (Elanchezhiyan et al., 2016). The bands are observed at 3618 $cm^{-1}$, 3406 $cm^{-1}$, 1627 $cm^{-1}$, 1033 $cm^{-1}$, and 786 $cm^{-1}$ in the FTIR spectra of BENT as shown in Figure 2b. The broad band at

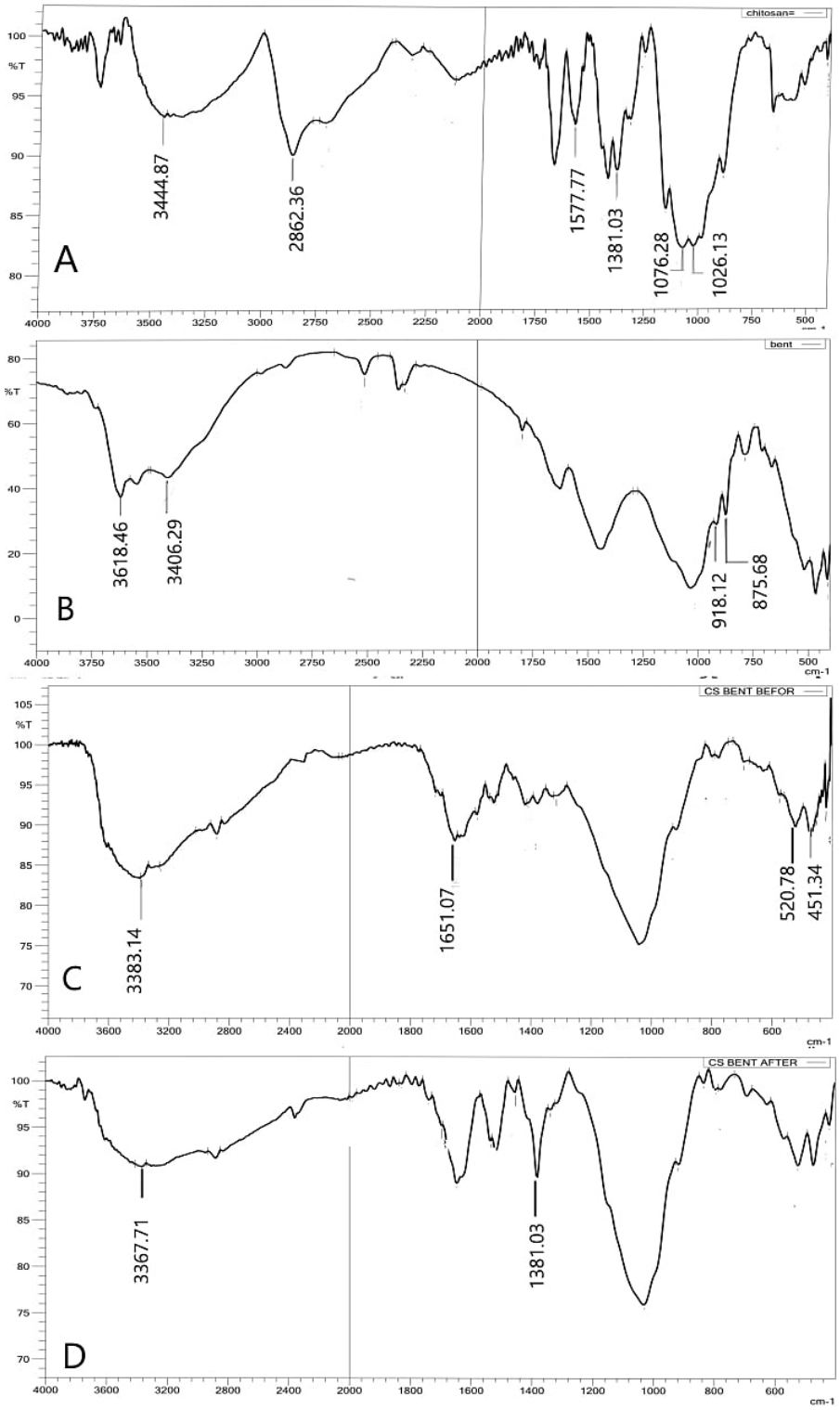


**Figure 2.** FTIR spectrum of (A) chitosan, (B) bentonite, (C) Cs-Bn-Zr beads before adsorption, and (D) Cs-Bn-Zr beads after adsorption

3406 $cm^{-1}$ is attributed to structural OH stretching, intermolecular hydrogen bonding, and water molecules in the clay material, demonstrating the hydroxyl linkage between octahedral and tetrahedral layers. The sharp band at 3618 $cm^{-1}$ is attributed to Si-OH stretching vibration (Pavithra et al., 2021). The wavenumber between 800 and 950 $cm^{-1}$ demonstrates the presence of the Si-O-Si, Al-O-Al, and Al-O-Si groups in BENT (Pavithra et al., 2021). Additionally, it can be observed from Figure 2c that the $Zr^{4+}$ ions were embedded into the composite beads by the Cs-Bn-Zr before adsorption peaks observed at 520 and 451 $cm^{-1}$ (Jiang et al., 2013) attributed to the Zr-N and Zr-O bonds, respectively. The bands at 1670 $cm^{-1}$ in chitosan shifted to 1651 $cm^{-1}$ in Cs-Bn-Zr beads, which was attributed to intermolecular interaction between chitosan's $-NH_2$ group. The band appeared at 3444 $cm^{-1}$ with chitosan reduced to 3383 $cm^{-1}$ in the Cs-Bn-Zr bead. However, Figure 2d demonstrated that this peak reduced to 3367 $cm^{-1}$ in Cs-Bn-Zr beads after adsorption, which may contribute to metal coordination with the chitosan functional groups (Banu et al., 2019). In addition, the spectra of beads after adsorption showed a new peak at 1381 $cm^{-1}$ (Nur et al., 2015), which was related to the N-O stretching frequency; this demonstrated that nitrate ions had been adsorbed on the adsorbent.

## Characterization by FESEM

FESEM images of Cs-Bn-Zr composite beads before and after nitrate ion adsorption are shown in Figure 3 (a to d). Zirconium was visible on the surface, as shown in Figure 3a. Before adsorption, the Cs-Bn-Zr beads in Figures (3b and 3c) showed high porosity and heterogeneity as an uneven rock-like structure resulting from chitosan intercalation on Bentonite surfaces. Because the nitrate-coated beads covered the porosity, they became less porous and smoother after adsorption, as shown in Figure 3d.

## EDX analysis

Figure 4 (a, b) shows the EDX characterization of Cs-Bn-Zr beads before and after nitrate ion adsorption. Bentonite was responsible for

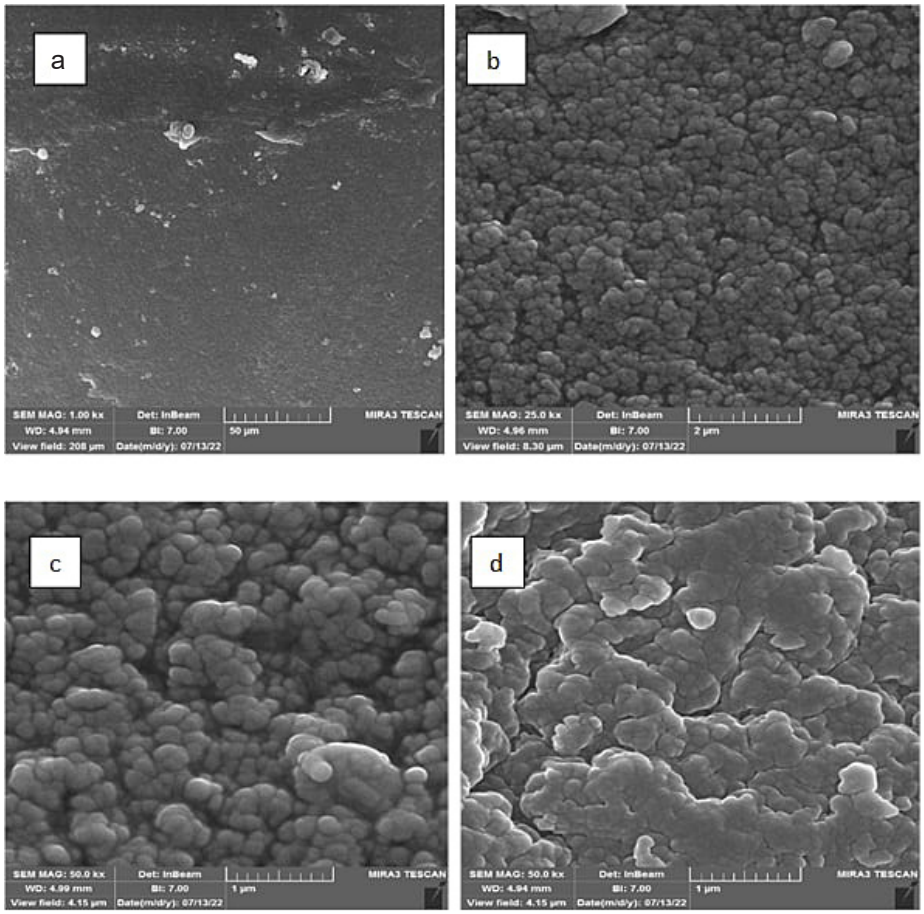


**Figure 3.** FESEM of (a, b, c) Cs-Bn-Zr beads before adsorption, (d) after nitrate adsorption

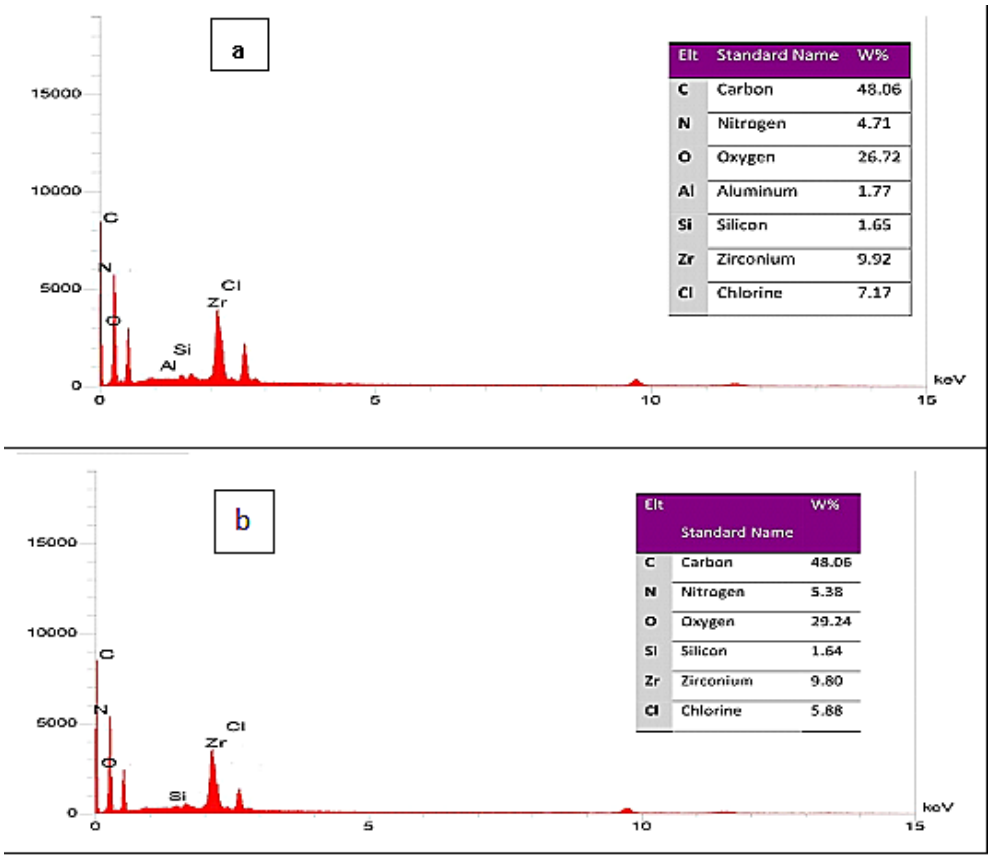


**Figure 4.** EDX of (a) Cs-Bn-Zr composite beads, (b) nitrate ion after adsorption on Cs-Bn-Zr composite beads

identifying the primary elements Si, O, and Al in the Cs-Bn-Zr composite. Chitosan recognized the primary elements C, N, and O, as demonstrated in Figure 4a. It can be observed from Figure 4b that the nitrogen and oxygen peaks increased in comparison with those obtained in Figure 4a, indicating that nitrate ions were adsorbed onto Cs-Bn-Zr beads. The peak of $Zr^{+4}$ emerged, demonstrating that the $Zr^{+4}$ had been successfully loaded onto the chitosan-bentonite beads. Furthermore, the chloride peak in Figure 4b was decreased, indicating that the sorption system also influenced the ion exchange mechanism.

## BET surface area analysis

The surface area of particles is evaluated using the (Brunauer, Emmett, and Teller) method. The surface area is a crucial parameter for enhancement of the mass transfer and provides more active sites. Table 1 displays that the surface areas of chitosan are (18.15 $m^2/g$) and the produced adsorbent (Cs-Bn-Zr) is (63.80 $m^2/g$). From the obtained values of surface area results, it can be concluded that the addition of bentonite increased the surface area of the chitosan-based bead.

**Table 1.** BET surface area analysis

| Adsorbents | Surface area $m^2/g$ |
|---|---|
| Chitosan powder | 18.15 |
| Cs-Bn-Zr composite beads | 63.80 |

## Effect of contact time

With an initial $NO_3$ concentration of 50 mg/L and an adsorbent dosage of (0.1 g), the impact of contact time on removal effectiveness and adsorption capacity was studied. According to Figure 5, contact time increases removal efficiency and adsorption capacity. By expanding the adsorption time from 30 minutes to 120 minutes, the removal efficiency grew considerably from 22% to 87%. However, the efficiency began to level off, and when the contact time was increased to 180 minutes, the efficiency only increased to 90.5%.

Adsorption capacity displayed a similar pattern of behavior, where increasing the contact time from 30 minutes to 120 minutes caused the adsorption capacity to rise steadily from 5.5 mg/g to 21.8 mg/g. The results show that when the contact period exceeded 120 minutes of contact time, the improvement in adsorption capacity

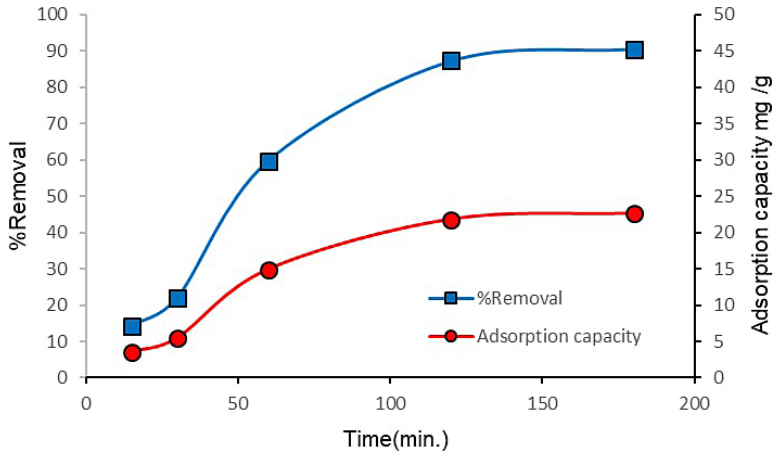


**Figure 5.** Effect of contact time on % removal and adsorption capacity

was negligible, peaking at roughly 22.6 mg/g at a contact time of 180 minutes. This pattern could be explained by the initial abundance of unused active sites in the process, followed by a minor restraint in adsorption capacity caused by the buildup of adsorbents (Karthikeyan et al., 2019c).

The outcomes of the current study are consistent with those attained by Ban et al. (2019). The results of this series of studies suggest that 120 minutes is the ideal operating duration for the adsorption process. At this point, both removal efficiency and adsorption capacity are at appropriate levels. Increasing the operating time beyond that point would be impracticable for the process. As a result, the remaining findings will be presented after 120 minutes of operation.

## Effect of initial concentration

Figure 6 shows how the initial concentration affects the elimination of nitrate. It is clear that raising the initial concentration from 50 to 800 mg/g at the adsorbent dosage of 0.1 g, rotation speed of 150, a contact time of 120 minutes and ambient temperature. the results domenstrated that the removal percentage droped from 87% to 26.65%. this could be due to the fact that at lower concentrations, the majority of the nitrate was adsorbed by Cs-Bn-Zr. Whereas at greater concentrations, the Cs-Bn-Zr was quickly saturable due to limited dosage and capacity.

On the other hand, the adsorption capacity exhibits a reversal reaction to that achieved with removal efficiency. With an initial $NO_3$ concentration of 600 mg/L, the adsorption capacity increased significantly from 21.8 mg/g with an initial concentration of 50 mg/g to roughly 110.46 mg/g.

This increase may be explained by a boost in the driving force produced by the gradient in nitrate concentration between the aqueous and solid phases. The results align with the work of Liu et al. (2016). At 600 mg/L, the adsorption

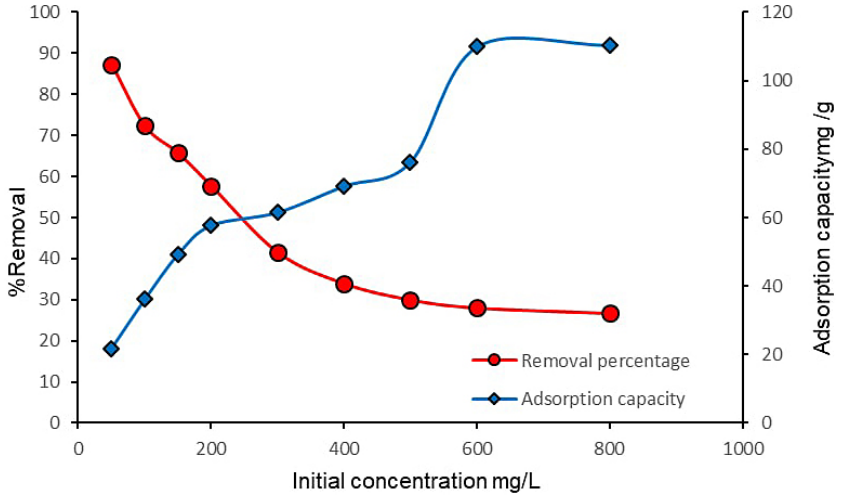


**Figure 6.** Effect of initial concentration on removal efficiency and adsorption capacity

capacity reaches a maximum of 110.46 mg/g, and then it flattens out, because the active sites of the adsorbed material are saturated with the pollutant.

## Effect of adsorbent dosage

The best adsorbent dosage might be obtained by varying the dosage (0.05, 0.1, 0.2, and 0.3 g) under the study conditions, such as a contact time of 120 minutes, 150 rpm, and 50 ml of nitrate concentration of 50 mg/L. The findings presented in Figure 7 showed that when the dosage of Cs-Bn-Zr was increased from (0.05 to 0.2 g), the removal was enhanced from 11 to 97 percent. The availability of increased surface area and adsorption functional sites with higher Cs-Bn-Zr dosage may cause this effect. Beyond 0.2 g, an additional increase in adsorbent dosage has no discernible impact on the removal efficiency. This behavior was in agreement with the results obtained by Liu et al. (2016). Therefore, 0.2 g was selected as the optimal dose for this study.

## Adsorption isotherm

The adsorption isotherm represents the equilibrium between the quantity of adsorbate that is adsorbed and that is in solution.

The experiments produced the most accurate adsorption statics. Nitrate adsorption statics onto Cs-Bn-Zr beads were determined by comparing Temkin's isotherm models to well-known isotherm models like Freundlich and Langmuir.

### *Langmuir isotherm model*

According to the Langmuir adsorption model, maximal adsorption corresponds to a saturated monolayer (chemical adsorption) of solute molecules on the adsorbent surface, with no transverse contact between the adsorbed molecules (Vijayaraghavan et al., 2006).

$$\frac{1}{q_e} = \frac{1}{q_{max}} + \frac{1}{q_{max}\, k_L}\, \frac{1}{c_e} \tag{3}$$

where: $q_e$ – the amount of nitrate adsorbed by adsorbent mass at equilibrium (mg/g);
$c_e$ – the concentration of nitrate (mg/L);
$k_L$ – Langmuir constant (L/mg);
$q_{max}$ – the maximal monolayer adsorption capacity (mg $NO_3$/g adsorbent).
Additionally, it was possible to explain the Langmuir isotherm using the separation factor ($R_L$) (Weber et al., 1974) that was determined using Equation (4):

$$R_L = \frac{1}{1 + k_L\, c_i} \tag{4}$$

where: $c_i$ – the initial concentration of nitrate (mg/L).
R's value indicates the sort of isotherm, with $R_L = 0$ being irreversible, $(0 < R_L < 1)$ being favorable, and $R_L = 1$ being unfavorable.

The plot of $\frac{1}{q_e}$ opposite $\frac{1}{c_e}$ was illustrated in Figure 8. The $q_{max}$ and $k_L$ were computed from the slope and intercept, respectively.

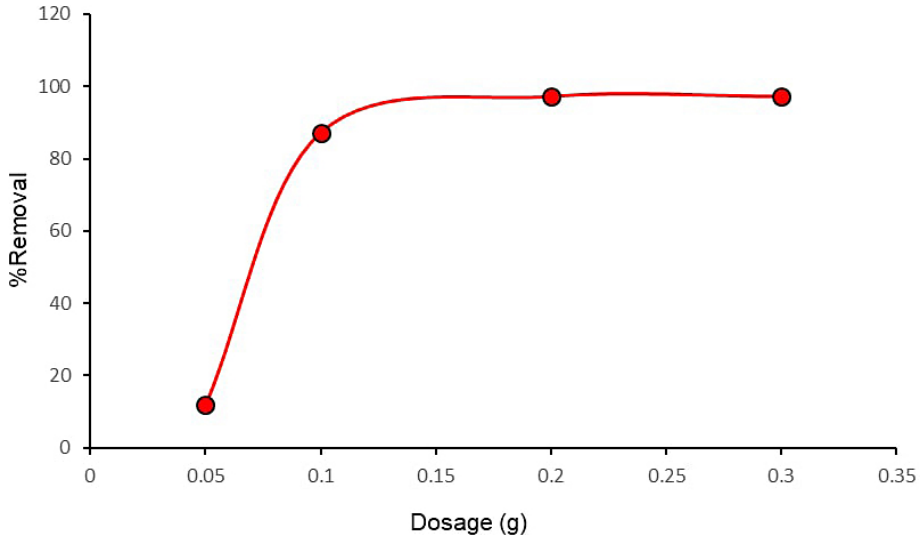


**Figure 7.** effect of adsorbent dosage on the removal efficiency

*Freundlich isotherm model*

The Freundlich model presupposed that the adsorption process takes place in multilayer sorption and that the molecular distribution on the surface of the adsorbent is heterogeneous (Shavandi et al., 2012). Freundlich's Equation is illustrated below in its linear form:

$$\log q_e = logk_f + \frac{1}{n} logc_e \quad (5)$$

where: $q_e$ (mg/g) – the amount of nitrate adsorbed by adsorbent mass at equilibrium; $c_e$ – the concentration of nitrate (mg/L); Freundlich empirical constants $k_f$ (mg/g) and $n$ serve as an indicator of adsorption capacity and favorability.

The plot of log $q_e$ opposite log $c_e$ is illustrated in Figure 9. The $\frac{1}{n}$, and $k_f$ were computed from the slope and intercept, respectively.

*Temkin isotherm model*

One characteristic of the Temkin isotherm makes good quality of the interaction between the adsorbent and adsorbate. Forms using this model were used and provided as Equation 6:

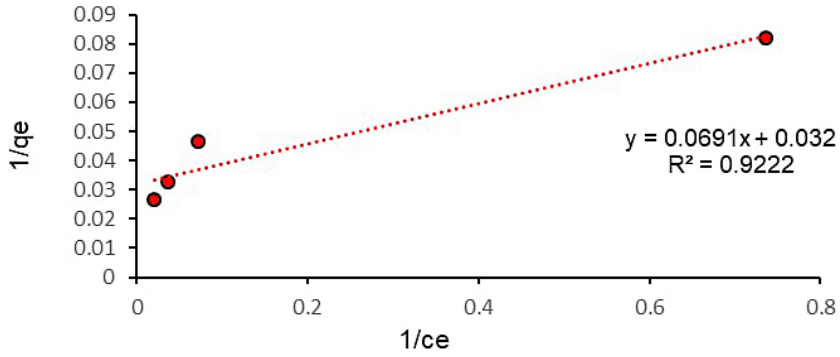


**Figure 8.** Langmuir adsorption isotherm of nitrate ions onto Cs-Bn-Zr

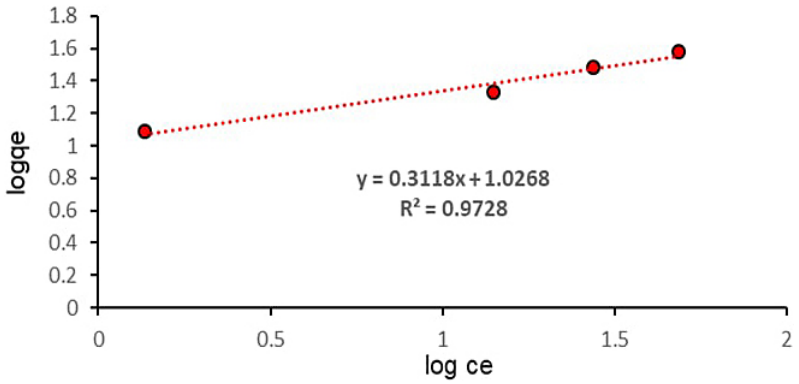


**Figure 9.** Freundlich adsorption isotherm of nitrate ions onto Cs-Bn-Zr

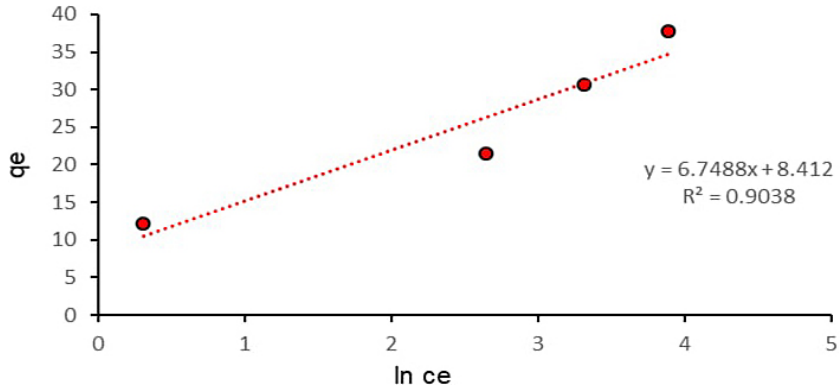


**Figure 10.** Temkin adsorption isotherm of nitrate ions onto Cs-Bn-Zr

**Table 2.** Parameter of Langmuir, Freundlich, and Temkin isotherm for nitrate ions

| Isotherm | Parameter | Value |
|---|---|---|
| Langmuir | $K_L$ (L/mg) | 0.463 |
| | $q_m$ (mg/g) | 31.25 |
| | $R^2$ | 0.9222 |
| | $R_L$ | 0.0414 |
| Freundlich | $K_F$ (mg/g) | 10.6365 |
| | 1/n | 0.3118 |
| | n | 3.2071 |
| | $R^2$ | 0.9728 |
| Temkin | $K_T$ (L/mg) | 3.4779 |
| | B | 6.7488 |
| | $R^2$ | 0.9038 |

$$q_e = Blnk_T + Blnc_e \quad (6)$$

where: $B$ – the Temkin constant;
$k_T$ – the Temkin isotherm constant (l/mg).

The plot of $q_e$ opposite ln $c_e$ is illustrated in Figure 10. Table 2 shows the values obtained for the Langmuir, Freundlich, and Temkin isotherm constants. With a correlation coefficient $R^2$ of (0.9728), it amply demonstrates the goodness of fit of experimental data of nitrate ion adsorption by Cs-Bn-Zr with the Freundlich model which indicate to multilayer adsorption. The size of the Freundlich coefficient $n$ provides a favorability measurement of the adsorption process. In the range, $n$ values between 2 and 10 indicate acceptable physical adsorption, between 1 and 2 moderate difficulties, and below 1 poor adsorption (Li et al., 2017; Radhi et al., 2021). This was supported by the results of the $n$ (3.2071) values obtained in the current study. This indicates significant physical adsorption.

## Adsorption kinetic

The kinetic analysis determines the solute uptake rate, which also establishes the amount of time that must pass before the adsorption reaction is complete (Sanyangare, 2016).

Two well-known kinetics adsorption models, the pseudo-second-order Equation and the pseudo-first-order Equationcan be used to determine the adsorption rate. The trials were carried out in various contact situations time. The linear form of the pseudo-first-order equation is as follows:

$$\ln(q_e - q_t) = lnq_e - k_1 t \quad (7)$$

where: $k_1$ – the pseudo-first-order constant (L/min);
$q_e$ and $q_t$ – the amounts of nitrate ions adsorbed at equilibrium and at any time, respectively (mg$No_3$/g adsorbent). Figure 11 shows the ln ($q_e$ - $q_t$) vs time graph.

The linear form of the pseudo-second-order equation demonstrates:

$$\frac{t}{q_t} = \frac{1}{k_2 q_e^2} + \frac{t}{q_e} \quad (8)$$

In Eq. (7), where $q_e$ and $q_t$ (mg/g) are defined, $k_2$ (g/mg. min) is the pseudo-second-order constant. Figure 12 shows the graph of $\frac{t}{q_t}$ Versus time.

According to Table 3, the correlation coefficients for the pseudo-first-order and pseudo-second-order were, respectively, (0.9755) and (0.816). In conclusion, the adsorption of nitrate ions by Cs-Bn-Zr was best characterized by the pseudo-first-order model. The pseudo-first order $q_{e,cal}$ (18.1 mg/g) was much closer to the experimental value (12.16 mg/g)

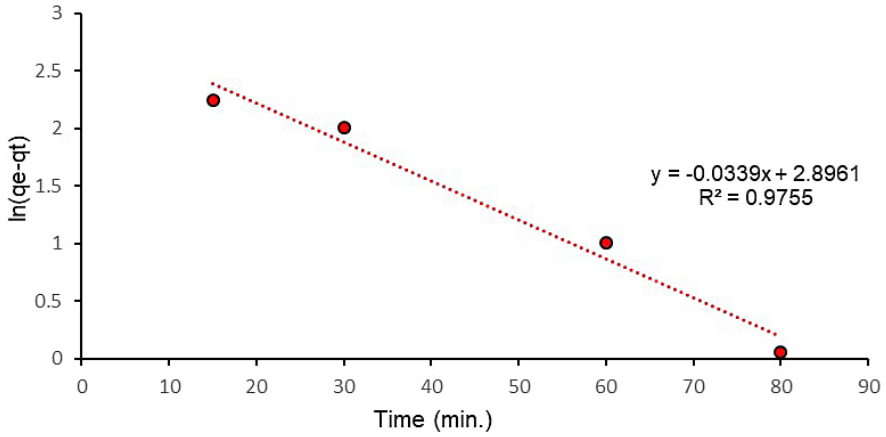


**Figure 11.** Pseudo-first-order kinetic model of nitrate ions

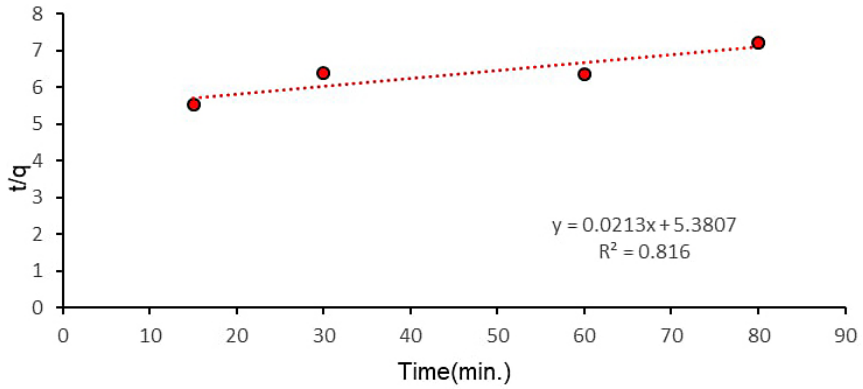


**Figure 12.** Pseudo-second-order kinetic model of nitrate ions

**Table 3.** Parameters of pseudo-first and second-order kinetics of nitrate ions

| Kinetic model | Parameter | Values | $R^2$ |
|---|---|---|---|
| 1st order | $q_{e.cal}$.mg/g | 18.1 | 0.9755 |
| | $q_{e.exp}$.mg/g | 12.16 | |
| | $k_1$ 1/min. | 0.0339 | |
| 2nd order | $q_{e.cal}$.mg/g | 46.94 | 0.816 |
| | $q_{e.exp}$.mg/g | 12.16 | |
| | $k_2$ g/mg.min | $8.43*10^{-5}$ | |

than the pseudo-second-order value. The pseudo-first-order kinetic process has been applied for reversible reactions, and an equilibrium between the liquid and solid phases has been achieved. At the same time, the pseudo-second-order kinetic model predicts that mass transfer is not the rate-limiting step but rather the adsorption mechanism.

## Regeneration process

The possibility of reuse of adsorbents is a significant consideration in the evaluation of adsorbents performance. To remove the nitrate from the adsorbent, 0.2 g of used (Cs-Bn-Zr) beads were immersed in 0.1 M NaCl solution in 50 ml for 90 minutes and shakingat 150 rpm. Then, filtered and rinsed several times with distilled water. Thereafter, the beads were air-dried at room temperature. The dried beads were subjected to an adsorption, adding 50 mL of a 600 mg/L nitrate solution and spinning the mixture at 150 rrpm for 120 minutes. The remaining nitrate concentration was analyed using a spectrophotometer. From the Figure 13, it can be observed that the

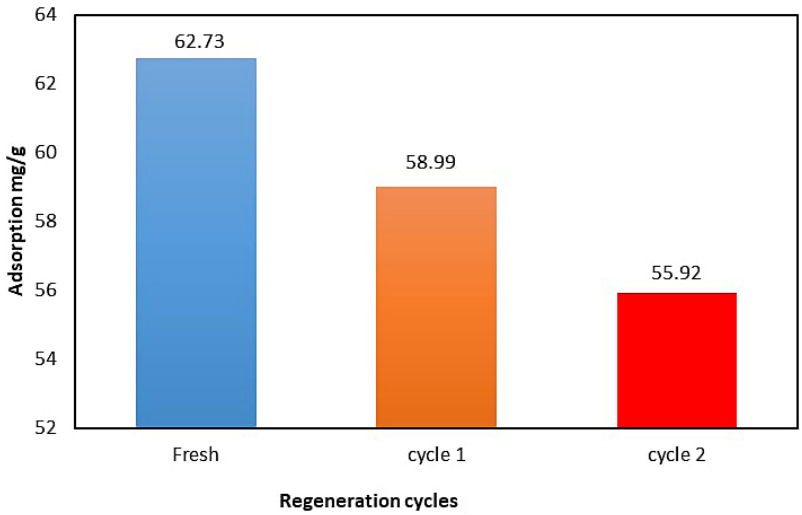


**Figure 13.** Regeneration process of Cs-Bn-Zr beads for the adsorption capacity of nitrate ions

nitrate adsorption capacity of Cs-Bn-Zr has not been significantly affected. After the first cycle of regeneration, the nitrate adsorption capacity of bead was found to be 58.99 mg/g. The second regeneration revealed that the adsorption capacity decreased to 55.92 mg/g. The results of regeneration test demonstrated the economic feasibility of Cs-Bn-Zr adsorbent in removal of nitrate.

### Adsorption mechanism

As shown in Figure 14, the proposed mechanism for removing nitrate by Cs-Bn-Zr is driven by electrostatic attraction and an ion exchange mechanism. Electrostatic forces caused Zr(IV), which is attached to amino groups in chitosan, to draw the oxy anions. Since nitrate ions exchange the Cl ions present in the Cs-Bn-Zr composite beads, which can be approved by the EDX spectrum, an ion exchange process was also involved.

### Comparative analysis

Table 4 shows that the adsorption capacity produced with Cs-Bn-Zr toward the nitrite was sufficient to conduct the removal process satisfactorily compared to the compression of modified chitosan adsorbent obtained in the prior research.

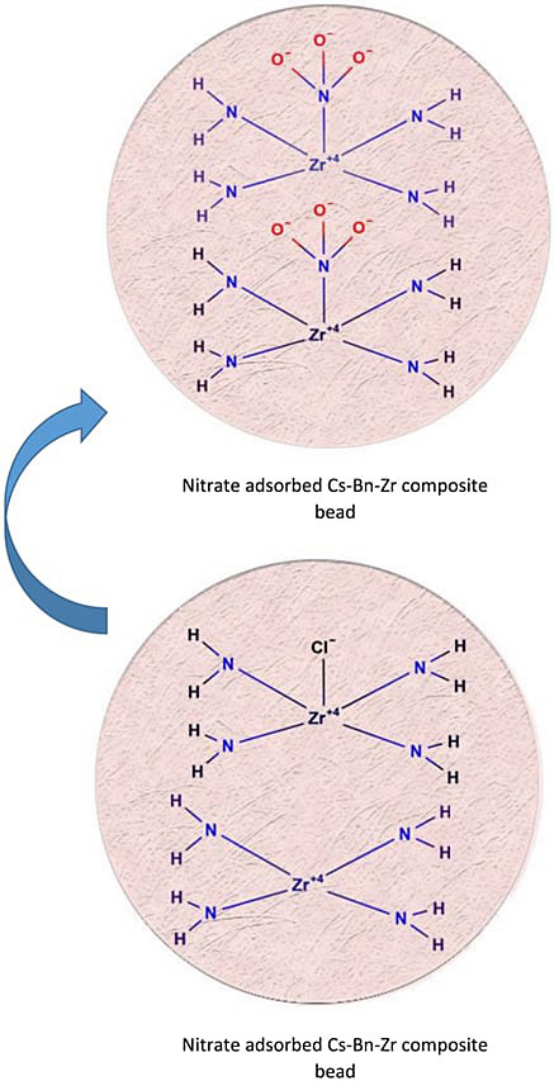


**Figure 14.** The proposed mechanism of removing nitrate by Cs-Bn-Zr beads

## CONCLUSIONS

In order to expand the surface area and selectivity of the adsorbent, Cs-Bn-Zr composite beads were produced. Zirconium was loaded onto the beads to improve the selectivity for nitrate anions, and bentonite was utilized to expand the surface area. FTIR, FESEM, EDX, and BET were used to analyze the (Cs-Bn-Zr) bead via the appropriate functional groups of beads (such as hydroxyl and amine). At 0.2 g of Cs-Bn-Zr optimal dosage at 2 hours with an initial concentration of 50 mg/l, the highest clearance percentage was 97.28%. The Freundlich isotherm model was

**Table 4.** A comparative study of Cs-Bn-Zr composite beads with other adsorbents to remove nitrate

| No. | Adsorbent | Initial concentration (mg/L) | Adsorption capacity (mg/g) | Ref. |
|---|---|---|---|---|
| 1 | Granular chitosan-Fe(III)-Al(III) complex | 150 | 8.58 | (Hu et al., 2016) |
| 2 | Chitosan-ethylene-glycol-hydrogel(CEGH) | 700 | 49.04 | (Chen et al., 2020) |
| 3 | Chitosan hydrogel beads | 1000 | 92.10 | (Chatterjee et al., 2009) |
| 4 | Local clay | 100 | 5.10 | (Battas et al., 2019) |
| 5 | $Fe_3O_4/ZrO_2/CS$ | 1-1000 | 89.3 | (Jiang et al., 2013) |
| 6 | Chitosan PVA composite | 10 mg/L | 30 .00 | (Rajeswari et al., 2016) |
| 7 | Fe-Cs-Alg. beads | - | 69.10 | (Karthikeyan et al., 2019 a) |
| 8 | Zn(II) loaded chitosan beads | 1000 | 59.00 | (Sowmya et al., 2015) |
| 9 | Chitosan-Bentonite-zirconium (Cs-Bn-Zr) | 600 | 110.46 | This study |

compatible with the nitrate adsorption isotherm on the surface of the Cs-Bn-Zr beads, demonstrating the multilayer adsorption. Nitrate ions behaved in pseudo-first order according to kinetic analyses, proving that physical adsorption was the rate-limiting step. Ion exchange, hydrogen bonding, and electrostatic attraction played significant roles in the adsorption mechanism.

## REFERENCES


1. Afkhami A. 2003. Adsorption and electrosorption of nitrate and nitrite on high-area carbon cloth: An approach to purification of water and waste-water samples. Carbon., 41, 1320–1322.
2. Ahmed M.J.,Hameed B.H.,Hummadi E.H. 2020. Review on recent progress in chitosan/chitin-carbonaceous material composites for the adsorption of water pollutants. Carbohydrate Polymers., 247, 116690.
3. Azlan K.,Wan Saime W.N., Lai Ken L. 2009. Chitosan and chemically modified chitosan beads for acid dyes sorption. Journal of Environmental Sciences., 21, 296–302.
4. Bae B.U., Jung Y.H., Han W.W., Shin H.S. 2002. Improved brine recycling during nitrate removal using ion exchange. Water Research., 36, 3330–3340.
5. Banu H.T., Karthikeyan P., Meenakshi S. 2019. Zr 4+ ions embedded chitosan-soya bean husk activated bio-char composite beads for the recovery of nitrate and phosphate ions from aqueous solution. International Journal of Biological Macromolecules., 130, 573–583.
6. Choudhary V.R.,Vaidya S.H. 1982. Adsorption of Copper Nitrate From Solution on Silica Gel. Journal of chemical technology and biotechnology, 32, 888–892.
7. Daneshvar E., Santhosh C., Antikainen E., Bhatnagar A. 2018. Microalgal growth and nitrate removal efficiency in different cultivation conditions: Effect of macro and micronutrients and salinity. Journal of Environmental Chemical Engineering, 6, 1848–1854.
8. Elanchezhiyan S.S., Sivasurian N., Meenakshi S. 2016. Enhancement of oil recovery using zirconium-chitosan hybrid composite by adsorptive method. Carbohydrate polymers, 145, 103–113.
9. Ghadiri S.K., Nasseri S., Nabizadeh R., Khoobi M., Nazmara S., Mahvi A.H. 2017. Adsorption of nitrate onto anionic bio-graphene nanosheet from aqueous solutions: Isotherm and kinetic study. Journal of Molecular Liquids, 242, 1111–1117.
10. Golden P.J., Weinstein R. 1998. Treatment of high-risk, refractory acquired methemoglobinemia with automated red blood cell exchange. Journal of clinical apheresis, 13, 28–31.
11. Hamid S.A., Shahadat M., Ismail S. 2017. Development of cost effective bentonite adsorbent coating for the removal of organic pollutant. Applied Clay Science, 149, 79–86.
12. Hammadi A., Shakir I. 2019. Adsorption Behavior of Light Naphtha Components on Zeolite (5A) and Activated Carbon. Iraqi Journal of Chemical and Petroleum Engineering, 20, 27–33.
13. Hasmath Farzana M., Meenakshi S. 2015. Photocatalytic aptitude of titanium dioxide impregnated chitosan beads for the reduction of Cr(VI). International Journal of Biological Macromolecules, 72, 1265–1271.
14. Herschy R.W. 2012. Water quality for drinking: WHO guidelines. Encyclopedia of Earth Sciences Series, 876–883.
15. Hu H.Y., Goto N., Fujie K. 2001. Effect of ph on the reduction of nitrite in water by metallic iron. Water Research, 35, 2789–2793.
16. Hummadi K.K. 2021. Optimal Operating Conditions for Adsorption of Heavy Metals from an Aqueous Solution by an Agriculture Waste. Iraqi Journal of Chemical and Petroleum Engineering, 22, 27–35.
17. Jiang H., Chen P., Luo S., Tu X., Cao Q., Shu M. 2013. Synthesis of novel nanocomposite Fe3O4/ZrO2/chitosan and its application for removal of nitrate and phosphate. Applied Surface Science, 284, 942–949.
18. Karthikeyan P., Banu H.A.T., Meenakshi S. 2019a. Synthesis and characterization of metal loaded chitosan-alginate biopolymeric hybrid beads for the efficient removal of phosphate and nitrate ions from aqueous solution. International journal of biological macromolecules, 130, 407–418.
19. Karthikeyan P., Banu H.A.T., Meenakshi S. 2019b. Removal of phosphate and nitrate ions from aqueous solution using La(3+) incorporated chitosan biopolymeric matrix membrane. International journal of biological macromolecules, 124, 492–504.
20. Karthikeyan P., Banu H.A.T., Meenakshi S. 2019c. Synthesis and characterization of metal loaded chitosan-alginate biopolymeric hybrid beads for the efficient removal of phosphate and nitrate ions from aqueous solution. International Journal of Biological Macromolecules, 130, 407–418.
21. Keshvardoostchokami M., Majidi M., Zamani A., Liu B. 2021. A review on the use of chitosan and chitosan derivatives as the bio-adsorbents for the water treatment: Removal of nitrogen-containing pollutants. Carbohydrate Polymers., 273, 118625.
22. Kumar I.A., Viswanathan N. 2017. Fabrication of metal ions cross-linked alginate assisted biocomposite beads for selective phosphate removal. Journal of Environmental Chemical Engineering, 5, 1438–1446.
23. Kyzas G.Z., Bikiaris D.N. 2015. Recent modifications of chitosan for adsorption applications: A critical and systematic review. Marine Drugs., 13, 312–337.

24. Li M., Lu B., Ke Q.F., Guo Y.J., Guo Y.P. 2017. Synergetic effect between adsorption and photodegradation on nanostructured TiO2/activated carbon fiber felt porous composites for toluene removal. Journal of Hazardous Materials, 333, 88–98.
25. Liu L., Ji M., Wang F. 2018. Adsorption of Nitrate onto $ZnCl_2$-Modified Coconut Granular Activated Carbon: Kinetics, Characteristics, and Adsorption Dynamics. (Majewski, P., Ed.)Advances in Materials Science and Engineering, 2018, 1939032.
26. Liu Q., Hu P., Wang J., Zhang L.,Huang R., 2016. Phosphate adsorption from aqueous solutions by Zirconium (IV) loaded cross-linked chitosan particles. Journal of the Taiwan Institute of Chemical Engineers., 59, 311–319.
27. Nur T., Shim W.G., Loganathan P., Vigneswaran S., Kandasamy J. 2015. Nitrate removal using Purolite A520E ion exchange resin: batch and fixed-bed column adsorption modelling. International Journal of Environmental Science and Technology, 12, 1311–1320.
28. Pavithra S., Thandapani G.S., Sugashini P., Sudha P.N., Alkhamis H.H., Alrefaei A.F., Almutairi M.H. 2021. Batch adsorption studies on surface tailored chitosan/orange peel hydrogel composite for the removal of Cr(VI) and Cu(II) ions from synthetic wastewater. Chemosphere, 271, 129415.
29. Purbasari A., Ariyanti D., Sumardiono S., Khairunnisa K., Sidharta T. 2022. Adsorption Kinetics and Isotherms of Cu(II) and Fe(II) Ions from Aqueous Solutions by Fly Ash-Based Geopolymer. Chemistry & Chemical Technology, 16, 169–176.
30. Radhi B.D., Mohammed W.T. 2021. Novel nanocomposite adsorbent for desulfurization of 4,6-dimethyldibenzothiophene from model fuel. Materials Today: Proceedings, 42, 2880–2886.
31. Rajeswari A., Amalraj A., Pius A. 2015. Removal of phosphate using chitosan-polymer composites. Journal of Environmental Chemical Engineering, 3, 2331–2341.
32. Raval H.D., Rana P.S., Maiti S. 2015. A novel high-flux, thin-film composite reverse osmosis membrane modified by chitosan for advanced water treatment. RSC Advances., 5, 6687–6694.
33. Rice E.W., Bridgewater L., Association A.P H., Association A.W.W., Federation W.E. 2012. Standard Methods for the Examination of Water and Wastewater. Standard Methods for the Examination of Water and Wastewater. American Public Health Association.
34. Saheed I.O., Oh W.D., Suah F.B.M. 2021. Chitosan modifications for adsorption of pollutants – A review. Journal of Hazardous Materials, 408, 124889.
35. Sanyangare F. 2016. Simulation of the Adsorptive Desulphurisation of Diesel Fuel. University of the Witwatersrand.
36. Shavandi M.A., Haddadian Z., Ismail M.H.S., Abdullah N., Abidin Z.Z. 2012. Removal of Fe (III), Mn (II) and Zn (II) from palm oil mill effluent (POME) by natural zeolite. Journal of the Taiwan institute of chemical engineers, 43, 750–759.
37. Sowmya A., Meenakshi S. 2014. Zr(IV) loaded cross-linked chitosan beads with enhanced surface area for the removal of nitrate and phosphate. International Journal of Biological Macromolecules, 69, 336–343.
38. Sulaymon A.H., Alhayali K.W., Waadallah A.A. 2010. Diffusion kinetics of Furfural adsorption onto Activated Carbon. Iraqi Journal of Chemical and Petroleum Engineering, 11, 21–27.
39. Vijayaraghavan K., Padmesh T.V.N., Palanivelu K.,Velan M. 2006. Biosorption of nickel (II) ions onto Sargassum wightii: application of two-parameter and three-parameter isotherm models. Journal of hazardous materials, 133, 304–308.
40. Wang Y., Gao B.Y., Yue W.W., Yue Q.Y. 2007. Adsorption kinetics of nitrate from aqueous solutions onto modified wheat residue. Colloids and Surfaces A: Physicochemical and Engineering Aspects, 308, 1–5.
41. Weber T.W., Chakravorti R.K. 1974. Pore and solid diffusion models for fixed-bed adsorbers. AIChE Journal, 20, 228–238.
42. Wu P.X., Liao Z.W., Zhang H.F.,Guo J.G. 2001. Adsorption of phenol on inorganic-organic pillared montmorillonite in polluted water. Environment International, 26, 401–407.